

Oxidative Degradation of Phenol via In-situ Generation of H_2O_2 in a Flow Reactor

Rong-Jian Li¹ · Richard J. Lewis¹ · Nicholas F. Dummer¹ · David J. Morgan^{1,2} · Ella Kitching³ · Thomas Slater³ · Graham J. Hutchings¹

Received: 9 September 2025 / Accepted: 12 October 2025 © The Author(s) 2025

Abstract

AuPd nanoalloys are shown to offer significantly enhanced catalytic performance for both the direct synthesis of hydrogen peroxide (H₂O₂) and the in-situ oxidative degradation of phenol. Under conditions where limited phenol conversion is observed using commercial H₂O₂, the bimetallic Au–Pd system facilitates efficient in-situ generation of H₂O₂ and associated reactive oxygen species (ROS), enabling phenol conversion rates exceeding 70%. By optimizing key reaction parameters, near-complete phenol degradation was achieved, alongside the effective breakdown of intermediate phenolic by-products. Notably, unlike earlier reported systems, the optimized 0.5%Au-0.5%Pd/TiO₂ catalyst exhibited excellent stability, maintaining consistent performance over 50 h of continuous operation, highlighting the potential to apply the in-situ approach for long-term application in advanced water treatment processes.

Rong-Jian Li and Richard J. Lewis are contributed equally to this work.

⊠ Richard J. Lewis
 LewisR27@Cardiff.ac.uk

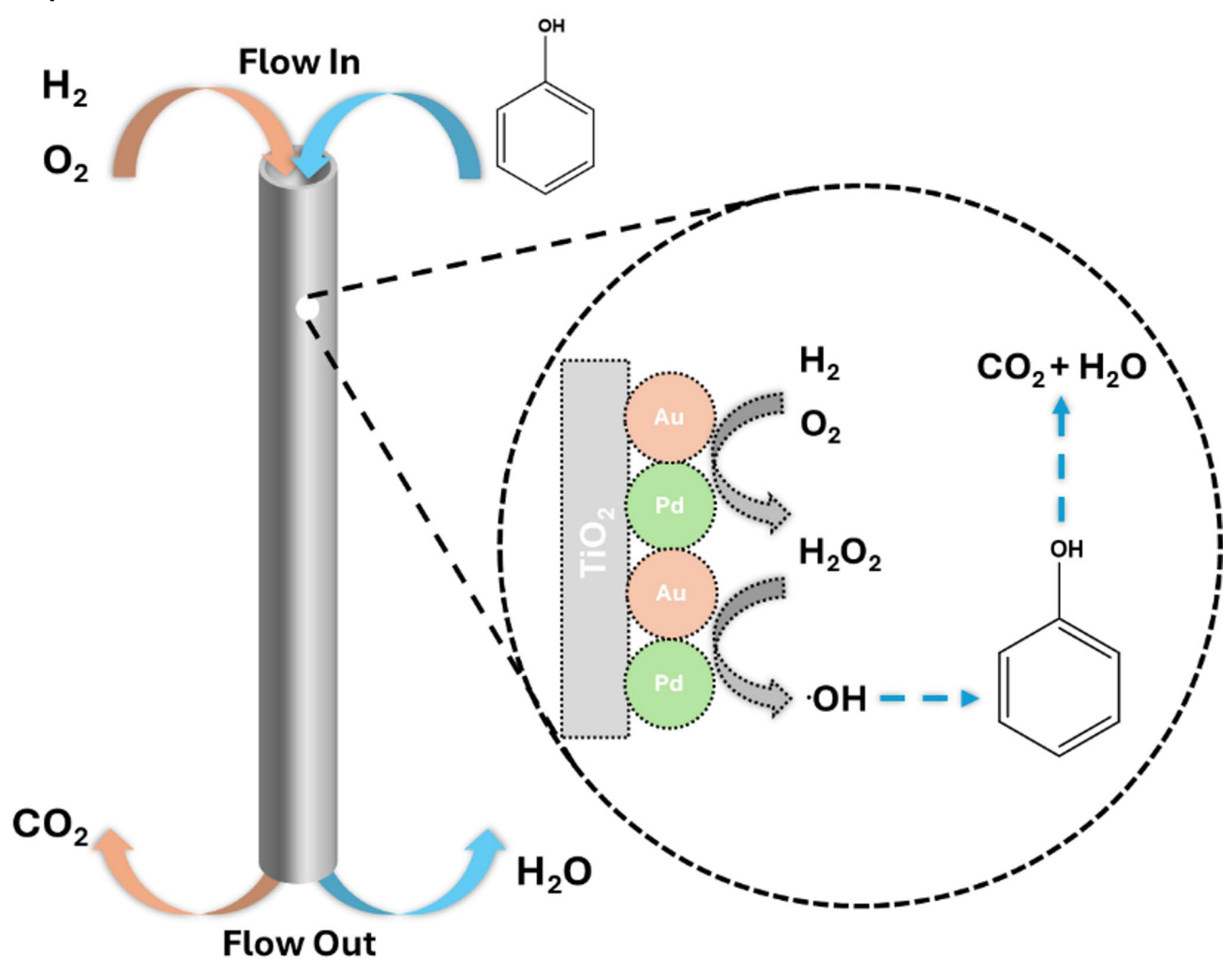
Published online: 23 October 2025

- ☐ Graham J. Hutchings Hutch@Cardiff.ac.uk
- Max Planck-Cardiff Centre on the Fundamentals of Heterogeneous Catalysis FUNCAT, Cardiff Catalysis Institute, School of Chemistry, Cardiff University, Translational Research Hub, Maindy Road, Cardiff CF24 4HQ, UK
- HarwellXPS, Research Complex at Harwell (RCaH), Didcot OX11 OFA, UK
- ³ School of Chemistry, Cardiff Catalysis Institute, Cardiff University, Cardiff CF24 4HQ, UK



373 Page 2 of 12 R.-J. Li et al.

Graphical Abstract



Keywords Phenol Oxidative Degradation · Gold-Palladium · Hydrogen Peroxide · Reactive Oxygen Species

Abbreviations

| ROS | Reactive oxygen species |
|---------|--|
| UV/Vis | Ultraviolet-visible |
| TCD | Thermal conductivity detector |
| PTFE | Polytetrafluoroethylene |
| HPLC | High-performance liquid chromatography |
| XPS | X-ray photoelectron spectroscopy |
| XRD | X-ray diffraction |
| ICDD | International Centre for Diffraction Data |
| TEM | Transmission electron microscopy |
| AC-STEM | Aberration-corrected scanning transmission |
| | electron microscopy |
| HAADF | high-angle annular dark field |
| EDX | Energy dispersive X-ray spectroscopy |
| ICP-MS | Inductively coupled plasma mass |

spectrometry

| Concentration |
|-------------------|
| Conversion |
| Selectivity |
| parts per billion |
| parts per million |
| |

1 Introduction

Phenolic compounds are widespread in industrial waste streams, including those from oil refineries, chemical and resin manufacturing, and the agricultural sector [1]. Traditional remediation methods, such as adsorption and incineration, produce large volumes of highly contaminated granular carbon beds, which not only raise handling and disposal concerns but also contribute significantly to greenhouse



gas (GHG) emissions [2]. Although there is growing interest in biological treatments [3–5] and advanced oxidation processes [6–8], their practical application remains questionable. Indeed, biological methods often have a limited operating window, especially in complex waste streams containing multiple pollutants [9, 10], while advanced oxidation techniques involve costly and potentially hazardous chemical reagents like ozone (O_3) [11] and hydrogen peroxide (H_2O_2) [12].

The use of in-situ generated H₂O₂, along with associated reactive oxygen species (ROS; \cdot OOH, \cdot OH, and \cdot O₂⁻), which are formed as intermediates during H₂O₂ generation, has emerged as a promising strategy for the degradation of phenolic compounds [13–17]. In contrast to alternative methods, including traditional Fenton-type systems that rely on homogeneous salts and commercial H₂O₂ (often resulting in significant sludge production) [18], the in-situ, heterogeneous approach enables the controlled formation of low concentrations of highly reactive oxidative species [16]. This not only enhances reaction efficiency but also eliminates the need for downstream treatment associated with residual metal salts or stabilizing additives commonly present in preformed H₂O₂ formulations [12]. Furthermore, the in-situ approach can be considered to offer greater compatibility with decentralized or continuous-flow treatment setups, reducing the need for chemical storage and minimizing secondary pollution. However, challenges remain in optimizing catalyst stability, with prior reports highlighting the limited stability of both noble metals (responsible for H₂O₂ generation) and non-noble, Fenton(-type) species (responsible for ROS generation), in the presence of highly oxidised products of phenol degradation (oxalic acid, formic acid, maleic acid, etc.) [14, 15, 17]. With these earlier works in mind, in this contribution, we explore the efficacy of AuPd-based catalysts, well reported in the literature for their efficacy in H₂O₂ synthesis, for the in-situ degradation of phenol, in a multiphase (gas-liquid-solid) flow system, with an aim to study key reaction parameters for effective degradation of this model contaminant.

2 Experimental

2.1 Catalyst Synthesis

A series of mono- and bi-metallic 1%AuPdTiO₂ catalysts were prepared (on a weight % basis), by an incipient wetness procedure. Our choice of TiO₂ support builds on earlier studies which have established the efficacy of TiO₂-based catalysts towards the direct synthesis of H₂O₂ [19] and the degradation of chemical pollutants via the in-situ approach

[14, 15]. The procedure to produce 0.5%Au-0.5%Pd/TiO₂ (10 g) is outlined below.

The TiO₂ (P25, Evonik) to liquid mass ratio of 5: 3.8 was predetermined, corresponding to 7.6 g of total liquid per 10 g of TiO₂. For the preparation of 10 g of 0.5%Au-0.5%Pd/ TiO₂ catalyst, appropriate amounts of solid HAuCl₄·3H₂O (0.1 g, ≥99.9% trace metals basis, Sigma-Aldrich) and PdCl₂ (0.083 g, 99.995% Pd by assay, Sigma-Aldrich), were first weighed separately into individual vessels. The precursors were subsequently combined and dissolved in a solution comprising of HCl (2.0 g, 37%, Fischer Scientific) and deionised water (5.52 g) to obtain a homogeneous AuPd precursor solution. Separately, TiO₂ (P25, 9.9 g, Evonik), was weighed and placed into a 250 mL glass beaker, and the precursor solution was gradually introduced, under continuous stirring using a glass rod. The resulting slurry was dried under at 60 °C for 12 h in a drying oven (under extraction), gently crushed to break down agglomerated particles and ground into a fine powder using an agate mortar and pestle. The powder was then chemically reduced using freshly prepared 5% hydrazine solution (prepared by diluting concentrated 35% hydrazine (Fischer Scientific) as required), by mixing 10 mL of the 5% hydrazine solution in 250 mL of deionised water. This reducing solution was added to the powder and stirred until a uniform dark navy or black colour developed, indicating complete reduction of Au and Pd species. The suspension was allowed to settle for 30 min, after which the supernatant was decanted. The resulting solid was washed (3 × 250 mL of deionised water), to remove residual hydrazine. Finally, the material was dried at 100 °C for 12 h, ground again to a fine powder, and subsequently pelletised to coarse powder (0.25–0.425 mm) prior to use.

2.2 Catalyst Testing

Note 1: Reaction conditions used within this study operate under the flammability limits of gaseous mixtures of H_2 and O_2 .

2.3 Direct Synthesis of H₂O₂

H₂O₂ synthesis was evaluated using a Parr Instruments stainless steel autoclave with a nominal volume of 50 mL, equipped with a PTFE liner, so that the total volume is reduced to 33 mL, and a maximum working pressure of 2000 psi. The autoclave liner was charged with catalyst (0.01 g) and H₂O (8.5 g, HPLC grade, Fischer Scientific). The charged autoclave was then purged three times with 5%H₂/N₂ (100 psi) before filling with 5%H₂/N₂ to a pressure of 420 psi, followed by the addition of 25%O₂/N₂ (160 psi), with the pressure of 5%H₂/N₂ and 25%O₂/N₂ given as gauge pressures. The reactor was not continually fed with



373 Page 4 of 12 R.-J. Li et al.

reactant gas. The reaction was conducted at room temperature of 20 °C for 0.5 h with stirring (1200 rpm). It should be noted that individual experiments were carried out, and the reactant mixture was not sampled on line.

To determine net $\rm H_2O_2$ concentration the solid catalyst was removed via filtration and an aliquot (2.0 mL) of the post reaction solution was combined with as prepared potassium titanium oxalate dihydrate (Sigma Aldrich) solution acidified with 30% $\rm H_2SO_4$ ([$\rm H_2SO_4$]=0.02 M, 2.0 mL) resulting in the formation of an orange pertitanic acid complex. This resulting solution was analysed spectrophotometrically using an Agilent Cary 60 UV/Vis Spectrophotometer at 400 nm by comparison to a calibration curve. Catalyst productivities are reported as $\rm mol_{H2O2}kg_{cat}^{-1}h^{-1}$.

The catalytic conversion of H_2 and selectivity towards H_2O_2 were determined using a Varian 3800 GC fitted with TCD and equipped with a Porapak Q column.

 H_2 conversion (Eq. 1) and H_2O_2 selectivity (Eq. 2) are defined as follows:

$$H_2O_2$$
 Selectivity (%) = $\frac{H_2O_2\text{detected (mmol)}}{H_2 \text{ consumed (mmol)}} \times 100$ (2)

The total autoclave capacity was determined via water displacement to allow for the accurate determination of H_2 conversion and H_2O_2 selectivity. When equipped with the PTFE liner, the total volume of an unfilled autoclave was determined to be 33 mL, which includes all available gaseous space within the autoclave.

2.4 Degradation of H₂O₂

Catalytic activity towards H₂O₂ degradation was determined in a similar manner to the direct synthesis activity of a catalyst. The autoclave liner was charged with solvent H₂O (7.82 g, HPLC grade, Fischer Scientific) and H₂O₂ (50 wt% 0.68 g, Sigma Aldrich), with the solvent composition equivalent to a 4 wt% H₂O₂ solution. From the solution, two 0.05 g aliquots were removed and titrated with an acidified Ce(SO₄)₂ solution using ferroin as an indicator to determine an accurate concentration of H₂O₂ at the start of the reaction. Subsequently, the catalyst (0.01 g) was added to the reaction media, and the autoclave was purged with 5%H₂/ N_2 (100 psi) before being pressurized with 5%H₂/N₂ (420 psi). The reaction medium was conducted at a temperature of 20 °C, and stirred (1200 rpm) for the desired reaction time, typically 30 min. After the reaction was complete, the catalyst was removed from the reaction mixture, and two 0.05 g aliquots were titrated against the acidified $Ce(SO_4)_2$

solution using ferroin as an indicator. The degradation activity is reported as $mol_{H2O2}kg_{cat}^{-1}h^{-1}$.

In all cases, reactions were run three times, over multiple batches of catalyst for the optimal formulation, with the data being presented as an average of these experiments. The catalytic activity toward the direct synthesis and subsequent degradation of H_2O_2 was found to be consistent to within $\pm 2\%$ on the basis of multiple reactions.

2.5 Phenol Degradation via the In-situ Synthesis of $\rm H_2O_2$

Catalytic activity towards the degradation of phenol was evaluated in our continuous fixed-bed reactor, equipped with a 1/8inch (3.2 inch outer diameter, with a catalyst bed of 1/4 inch (6.4 mm). A typical phenol degradation reaction was carried out using 0.12 g of the 1%AuPd/TiO2 catalyst, which had been pressed (10 T, 30 s) into a disc and sieved to a particle size of 0.25–0.425 mm. The granulated catalyst was mixed with SiC powder (4.1 g, approximately 0.37 mm particle size, Fischer Scientific), and supported at the bottom of the catalyst bed in the reactor tube by glass wool. The catalyst and diluent were contained within a 10 cm stainless-steel tube with a 1/4 inch (6.4 mm) outer diameter. The reactor system was then pressurized, typically to 10 bar, and at a temperature of 20 °C. When the reactor had reached the required pressure and the flow through the system had stabilized, the phenolic solution (10 ppm phenol in H₂O, HPLC grade), was introduced into the reactor, typically at a flow of 0.2 mL min⁻¹ using an Agilent 1290 Infinity HPLC pump. Total gas flow rates (typically 42 mLmin⁻¹, $5\%H_2/N_2$: 35 mLmin⁻¹, and 25%O₂/N₂: 7 mLmin⁻¹), were controlled using mass flow controllers, and one-way valves were placed after the mass flow controllers to prevent any liquid from entering them during the reaction. The reactor pressure was maintained using a back-pressure regulator at the end of the system, and pressure relief valves were included at various points throughout the system. Aliquots of post-reaction solutions were collected and analysed using high-performance liquid chromatography (HPLC) fitted with an Agilent Poroshell 120 SB-C18 column.

Where possible, phenol oxidation product distribution has been grouped into two categories, namely the phenolic derivatives (catechol, hydroquinone, resorcinol, and benzoquinone) and others, which include the organic acids (formic acid, acetic acid, fumaric acid, maleic acid, malonic acid, muconic acid, and oxalic acid), water, and carbon dioxide (i.e., the products of total oxidation). Note that while it is possible for the completed oxidation of phenol to occur, the presence of water as a reaction medium prevented the detection of this product. Further, we were unable to



analyse post-reaction gas streams due to equipment limitations, which prevented the quantification of CO₂.

Phenol conversion (Eq. 3), selectivity towards phenolic derivatives (PD) (Eq. 4) or others (organic acids, CO_{2} , and H_2O) (Eq. 5) are defined as follows:

Phenol Conversion (%)
$$= \frac{\text{mmol}_{\text{Phenol } (t(0))} - \text{mmol}_{\text{Phenol } (t(1))}}{\text{mmol}_{\text{Phenol } (t(0))}} \times 100$$
(3)

Selectivity towards PD (%) =
$$\frac{\text{mmol}_{\text{PD}}}{\text{mmol}_{\text{phenol converted}}} \times 100$$
 (4)

Selectivity towards others (%)

$$= \frac{mmol_{phenol(t(1))} - mmol_{PD(t(1))}}{mmol_{phenol(t(1))}} \times 100$$
 (5)

To probe the contribution of alternative pathways to phenol conversion (i.e., via aerobic or reductive pathways), an identical procedure to that outlined above for the oxidative degradation of phenol was followed, with the reactor charged with $5\%H_2/N_2$ or $25\%O_2/N_2$ reagent gases. Additionally, experiments were conducted using preformed H_2O_2 (100 ppm). Further studies were conducted in the presence of the radical quenching agent t-butanol (TBA), at a concentrations of 100 ppm.

2.6 Catalyst Characterization

X-ray photoelectron spectroscopy (XPS) measurements were performed on a Kratos Axis Ultra-DLD photoelectron spectrometer utilising a monochromatic Al K_a X-ray source operating at 144 W (12 mA × 12 kV). Samples were pressed onto silicone-free double-sized Scotch tape, and analysed using the hybrid spectroscopy mode, giving an analysis area of ca. 700 × 300 microns. High resolution and survey spectra were acquired at pass energies of 40 eV (step size 0.1 eV) and 160 eV (step size 1 eV), respectively. Charge compensation was performed using low-energy electrons, and the resulting spectrum was calibrated to the lowest C(1s) peak from the fitted carbon core-level spectra, taken to be 284.8 eV. The suitability of the C(1s) referencing was confirmed by a secondary reference point, taken to be the Ti(2p_{3/2}) peak with a binding energy of 458.7 eV, characteristic of that for virgin TiO₂. All data were processed using CasaXPS v2.3.24 using a Shirley background and modified Wagner factors as supplied by the instrument manufacturer. Peak fits were performed using a combination of Voigt-type functions (LA line shape in CasaXPS) and models derived from bulk reference samples where appropriate.

The bulk structure of the catalysts was determined by powder X-ray diffraction (XRD) using a $(\theta-\theta)$ PANalytical

X'pert Pro powder diffractometer using a Cu K_{α} radiation source, operating at 40 keV and 40 mA. Standard analysis was carried out using a 40 min run with a back-filled sample, between 20 values of $20-80^{\circ}$. Phase identification was carried out using the International Centre for Diffraction Data (ICDD).

Transmission electron microscopy (TEM) was performed on a JEOL JEM-2100 operating at 200 kV. Samples were prepared by powder dispersion and then deposited on 300 mesh copper grids coated with holey carbon film. To allow for the determination of mean particle size, a minimum of 300 particles was measured. Aberration-corrected scanning transmission electron microscopy (AC-STEM) was performed using a probe-corrected ThermoFisher Spectra 200 S/TEM operating at 200 kV and a convergence semiangle of 29.5 mrad. High spatial resolution STEM imaging was acquired with a high-angle annular dark field (HAADF) detector, an inner collection angle of approximately 56 mrad (outer angle of approximately 200 mrad). Energy dispersive X-ray spectroscopy (EDX) was performed using a Thermo-Fisher Super-X detector, and the data were analysed using Thermo Scientific Velox Software.

Total metal leaching from the supported catalyst under in-situ phenol degradation conditions, was quantified via inductively coupled plasma mass spectrometry (ICP-MS). Post-reaction solutions were analysed using an Agilent 7900 ICP-MS equipped with I-AS auto-sampler. All samples were diluted by a factor of 10 using HPLC grade H₂O (1% HNO₃ and 0.5% HCl matrix). All calibrants were matrix-matched and measured against a five-point calibration using certified reference materials purchased from Perkin Elmer and certified internal standards acquired from Agilent.

To allow for the quantification of total metal loading the as-prepared catalysts were digested via an aqua-regia assisted microwave digestion method using a Milestone Connect Ethos UP microwave with an SK15 sample rotor. Digested samples were analysed by (ICP-MS). All calibrants were matrix-matched and measured against a five-point calibration using certified reference materials purchased from Perkin Elmer and certified internal standards acquired from Agilent.

3 Results and Discussion

The introduction of Au into supported Pd nanoparticles has been well studied for a range of oxidative transformations, with the formation of AuPd nanoalloys often offering considerable enhancements in reactivity, selectivity, and stability compared to their monometallic analogues. Typically, these improvements are attributed to 'synergistic effects,' a catch-all term that encompasses electronic and structural



373 Page 6 of 12 R.-J. Li et al.

Table 1 Metal loading of the as-prepared Au-Pd/TiO₂ catalysts, as established by ICP-MS analysis of aqua-regia digested samples

| Catalyst Formulation | Actual Au loading/ | Actual Pd |
|--|--------------------|-------------|
| | wt% | loading/wt% |
| 1%Au/TiO ₂ | 1.00 | _ |
| $0.75\% \mathrm{Au}\text{-}0.25\% \mathrm{Pd/TiO}_2$ | 0.72 | 0.24 |
| $0.5\% \mathrm{Au}\text{-}0.5\% \mathrm{Pd/TiO}_2$ | 0.43 | 0.46 |
| $0.25\% \mathrm{Au}\text{-}0.75\% \mathrm{Pd/TiO}_2$ | 0.28 | 0.76 |
| 1%Pd/TiO ₂ | _ | 0.96 |

Table 2 Particle size of 1%AuPd/TiO₂ catalysts as determined by TEM

| Catalyst Formulation | Particle Diameter/nm (S.D) |
|--|----------------------------|
| 1%Au/TiO ₂ | 10.5 (8.3) |
| $0.75\% \mathrm{Au}\text{-}0.25\% \mathrm{Pd/TiO}_2$ | 6.5 (3.9) |
| 0.5%Au- $0.5%$ Pd/TiO ₂ | 6.1 (2.8) |
| $0.25\% \mathrm{Au}\text{-}0.75\% \mathrm{Pd/TiO}_2$ | 4.5 (1.8) |
| 1%Pd/TiO ₂ | 4.8 (2.1) |

Table 3 Au: Pd atomic ratio of 1%AuPd/TiO $_2$ catalysts as determined by XPS analysis

| Catalyst Formulation | Pd: Au | $Pd^{2+}:Pd^0$ | |
|--|--------|---------------------|--|
| 1%Au/TiO ₂ | _ | _ | |
| 0.75%Au-0.25%Pd/TiO ₂ | 1.50 | 0.13 | |
| 0.5%Au-0.5%Pd/TiO ₂ | 2.40 | 0.17 | |
| $0.25\% \mathrm{Au}\text{-}0.75\% \mathrm{Pd/TiO}_2$ | 9.00 | All Pd ⁰ | |
| 1%Pd/TiO ₂ | _ | All Pd ⁰ | |

changes, which result from the formation of bimetallic species [20–22]. The use of in-situ synthesised H₂O₂ and associated reactive oxygen species in chemical valorisation represents areas of growing interest, where the synergy that results from Au-Pd alloy formation has been exploited to a considerable degree [23, 24]. Building on these earlier works, we now turn our attention to the application of a series of AuPd-based catalysts, immobilised on a TiO₂ (P-25) carrier, for the in-situ degradation of phenol, a widely studied model contaminant [25].

Prior to their application in the oxidative degradation of phenol, the catalyst series was extensively characterised in order to identify potential structural-reactivity relationships. As expected with the impregnation method used for catalyst synthesis, the actual loadings of Au and Pd in the prepared formulations were close to their nominal values (Table 1).

With a strong correlation between catalytic selectivity and nanoparticle size well known [26], we subsequently probed active site dispersion by X-ray diffraction (XRD) (Figure S.1). No clear reflections associated with Au or Pd were observed, which may indicate high dispersion or merely be a result of the relatively low loading of metals on the catalyst surface. To provide a further indication of particle size, transmission electron microscopy (TEM) was employed, with mean particle diameters reported in Table 2 (associated particle size distribution and micrographs are reported in Figure S.2–3). A clear correlation between mean

particle size and catalyst formulation was observed, with the Au-rich formulations consisting of larger species compared to the Pd-rich analogues, aligning well with earlier studies into AuPd-based materials prepared by a similar impregnation protocol [27].

Further analysis via X-ray photoelectron spectroscopy (XPS) (Figure S.4, with elemental surface ratios reported in Table 3) reveals that the formation of AuPd alloys significantly modifies Pd-oxidation state, with a shift towards Pd²⁺ observed with the introduction of relatively large quantities of Au (i.e. at Au loadings≥0.5wt.%). Notably Au is found to exist purely in the metallic state, with no cationic species observed (Figure S.5).

With the catalyst series extensively characterised we subsequently set out to investigate the efficacy of these materials towards the direct synthesis and subsequent degradation of H₂O₂, under reaction conditions considered sub-optimal for H₂O₂ production (i.e. in a batch regime, under ambient temperature and in the absence of the alcohol co-solvent typically utilised to promote H₂O₂ stability and gaseous reagent solubility), but relevant to the real world oxidative treatment of aqueous waste-streams (Table 4). In keeping with earlier works, the incorporation of Au into a supported Pd catalyst was found to improve catalytic performance towards H₂O₂ production [27–29], with accumulated H_2O_2 concentrations (from 20 to 53 ppm), observed over the bimetallic series, greater than that offered by the Pd-only (12 ppm) and Auonly (6 ppm) catalysts after 30 min of reaction. Notably, this improved performance can be related to enhancements in catalytic selectivity (6-19% H₂O₂ selectivity in the case of the bimetallic catalysts), rather than increased reactivity/H₂ utilization, as indicated by the near identical H₂ conversion rates (between 2 and 5%) observed over these formulations.

 $\rm H_2O_2$ direct synthesis reaction conditions: catalyst (0.01 g), $\rm H_2O$ (8.5 g), 5% $\rm H_2/N_2$ (420 psi), 25% $\rm O_2/N_2$ (160 psi), 0.5 h, 20 °C, 1200 rpm. $\rm H_2O_2$ degradation reaction conditions: catalyst (0.01 g), $\rm H_2O_2$ (50 wt% 0.68 g), $\rm H_2O$ (7.82 g), 5% $\rm H_2/N_2$ (420 psi), 0.5 h, 20 °C, 1200 rpm.

Building on these studies, we subsequently evaluated the performance of the catalyst series towards the oxidative degradation of phenol, via the in-situ synthesis of H_2O_2 and associated reactive oxygen species (ROS; ·OOH, ·OH, O_2^-), with these latter species considered to be generated as intermediates during H_2O_2 synthesis or via subsequent degradation of H_2O_2 [16]. A schematic of the flow reactor designed to evaluate catalytic performance is shown in Figure S.6.A, with a photograph of the reactor shown in Figure S.6.B. We first established the negligible ability of the catalyst diluent (SiC, 4.1 g) to promote the degradation of H_2O_2 (Figure S.7), or act as a sequestering agent for phenol (Figure S.8), with a limited degree of phenol adsorption observed



Table 4 The effect of au: Pd ratio on the activity of 1%AuPd/TiO₂ catalysts towards the direct synthesis and subsequent degradation of H₂O₂

| Catalyst | H ₂ O ₂ Productivity/mol _{H2O2} kg _{cat} ⁻¹ h ⁻¹ | H ₂ O ₂ Conc./ ppm | H ₂ Conv./% | H ₂ O ₂ Sel./% | H ₂ O ₂ Degradation/ mol _{H2O2} kg _{cat} ⁻¹ h ⁻¹ (%) |
|--|--|---|---------------------------|---|--|
| 1%Au/ TiO ₂ | 0.3 | 6 | 1 | 6 | 0 (0) |
| 0.75%Au- 0.25%Pd/ TiO ₂ | 2.6 | 53 | 3 | 19 | 683 (33) |
| 0.5%Au- 0.5%Pd/ TiO ₂ | 2.5 | 50 | 4 | 14 | 650 (32) |
| 0.25%Au- 0.75%Pd/ TiO ₂ | 1.0 | 20 | 4 | 6 | 799 (39) |
| 1%Pd/ TiO ₂ | 0.6 | 12 | 5 | 2 | 595 (28) |

initially (5% at a reaction time of 0.5 h), with no additional adsorption (< 1%) at extended reaction times.

Subsequently, we set out to establish the efficacy of the series of 1%AuPd/TiO₂ catalysts towards the in-situ oxidative degradation of phenol (Fig. 1A). A clear enhancement in reactivity was observed upon the formation of AuPd nanoalloys, with the bimetallic catalysts (68–80% phenol conversion) outperforming the monometallic analogues (58 and 2% for the 1%Pd/TiO₂ and 1%Au/TiO₂ catalysts, respectively) upon reaching steady state. The activity of the 0.25%Au-0.75%Pd/TiO₂ formulation is particularly noteworthy, achieving rates of phenol conversion over 80%. These observations are further supported by our evaluation of a physical mixture of the monometallic materials (Fig. 1B), which achieves phenol degradation rates (56%) comparable to the sum of the individual components (54%), and inferior to the bimetallic analogue (73%), evidencing the enhanced performance which results from the formation of AuPd alloys.

With a focus on the bimetallic 0.5%Au-0.5%Pd/TiO₂ catalyst we established the significant improvement in oxidative degradation which may be achieved from the in-situ generation of H2O2 (and associated ROS), with relatively limited conversion observed when using either molecular H₂ (20% phenol conversion), or O₂ (< 1% phenol conversion) alone (Fig. 1C). With the incomplete purging of dissolved oxygen from the reaction medium and the resulting production of low concentrations of H₂O₂, and related radical species, considered the primary cause for the observed conversion under a H₂ only atmosphere [15]. Subsequent studies also indicated that a significant improvement in phenol conversion may be obtained via in-situ H₂O₂ production, compared to that observed when using the preformed oxidant (< 0.5% coversion when co-feeding 100 ppm H₂O₂), with these latter experiments further implicating oxidative species other than H₂O₂ as primarily responsible for the observed reactivity (Fig. 1C). Further, support for the key role of ROS, rather than H₂O₂, in the oxidative degradation of phenol is provided from radical quenching experiments where a substantial decrease in phenol conversion was observed in the presence of t-butanol, a widely utilized scavenger for O-based radical species (Figure S.9). Taken alongside our earlier works into the in-situ approach to water disinfection, which evidenced the release of highly potent O-based radical species, in addition to H₂O₂, from Au-Pd surfaces during H₂O₂ synthesis [16] we are able to hypothesise that, while there may be a minimal contribution to phenol degradation from ROS generated from the catalytic cleavage of H₂O₂ (e.g. via Fenton-type pathways), H_2O_2 is not the key species primarily responsible for phenol degradation. Rather we consider that these studies implicate the intermediates generated on the way to H₂O₂ are primarily responsible for the observed oxidation.

Importantly, for all catalysts, we observe no significant loss in catalyst performance over several hours on-stream, which aligns well with our analysis of post-reaction solutions by ICP-MS (Table S.1). The stability of Au in particular is noteworthy, with a small degree of Pd lost ($\leq 0.3 \,\mu g L^{-1}$) after 30 min of reaction. However, no further Pd leaching was observed at extended reaction times. Indeed, with a particular focus on the 0.5%Au-0.5%Pd/TiO₂ catalyst, we have established catalyst stability towards long-term insitu phenol degradation, with a phenol degradation rate in excess of 70% maintained up to 50 h on-stream (Fig. 1D), with ICP-MS analysis (Table S.2) indicating no detectable leaching of either precious metal at extended reaction times. Comparison between fresh and used samples by STEM-EDX revealed that the bimetallic nanoparticle composition observed in the fresh material was largely retained after 50 h on-stream (Fig. 2A, B). Notably, we observe a degree of aggregation into chain-like structures observed after exposure to reaction conditions (i.e. after 50 h on-stream) and evidence of the formation of small Pd-only nanoparticles, after relatively short reaction times (with analysis performed



373 Page 8 of 12 R.-J. Li et al.

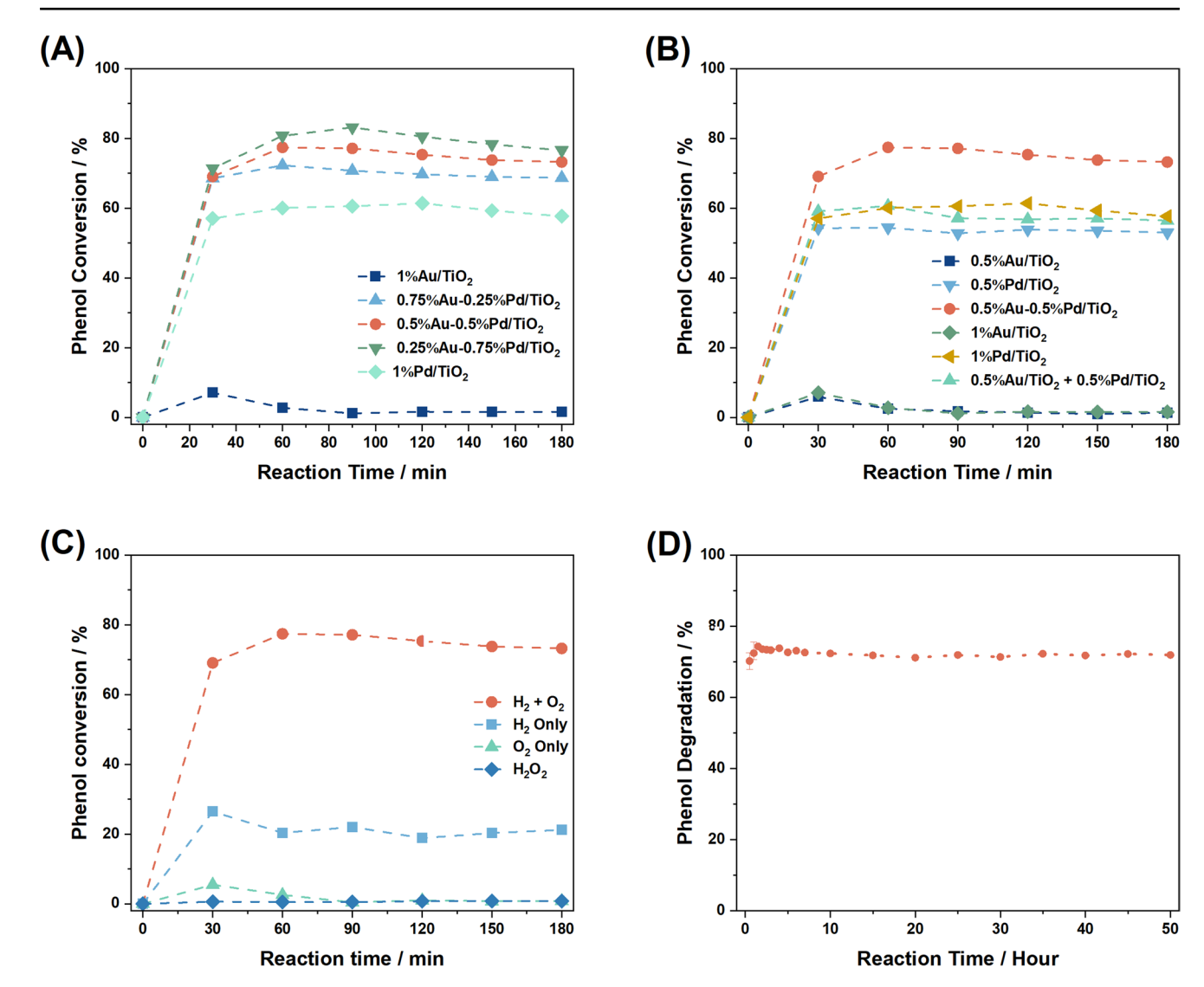


Fig. 1 The performance of $1\%\text{AuPd/TiO}_2$ catalysts towards the degradation of phenol via the in-situ production of H_2O_2 . A The effect of Au: Pd ratio on catalytic reactivity. B The requirement for Au-Pd alloys as established by comparison between bimetallic formulations and a physical mixture of monometallic analogues. C Control experiment

demonstrating the contribution of the different reactants (H_2 , O_2 and H_2O_2 (100 ppm)). **D** The long-term stability of the 0.5%Au-0.5%Pd/TiO₂ catalyst. Reaction conditions: catalyst (0.12 g), SiC (4.1 g), phenol solution (10 ppm, in H_2O), total gas flow rate: 42 mLmin⁻¹ ($H_2:O_2=1$), 10 bar, liquid flow rate: 0.2 mLmin⁻¹, 20 °C

after 3 h of reaction) (Figure S.10). The aggregation appears to have very limited effect on catalytic performance, and we reiterate the continued presence of bimetallic particles after use. However, such analysis does indicate the need for further efforts to improve catalyst stability if the in-situ approach is to find large-scale application. We recognise that phenol conversion alone is a relatively crude indicator of catalyst stability and in light of the dynamic nature of the immobilised species on-stream, as indicated by our analysis by electron micrscopy, and consider that further efforts are required to establish how such variation in nanoparticle size and composition dictate more nuanced indicators of catalyst stability, including ROS speciation (and quantity) and H₂ conversion.

Further analysis of the spent catalyst by XPS (Figure S.11, with elemental surface ratios in Table S.3), shows no meaningful changes in Pd oxidation state after 50 h onstream, with the Pd²⁺/Pd⁰ ratio comparable to that observed in the as-prepared catalyst. Similarly, the Au: Pd surface atomic ratios for the fresh, used (50 h) samples are indistinguishable within quantification uncertainty, implying no measurable metal leaching which is consistent with our previous ICP-MS analysis.

In attempt to improve phenol conversion rates, we subsequently set out to optimise reaction conditions, including gas and liquid flow rates, pressure, substrate concentration, and catalyst loading (Fig. 3A–D). A clear inverse correlation was found to exist between phenol conversion and



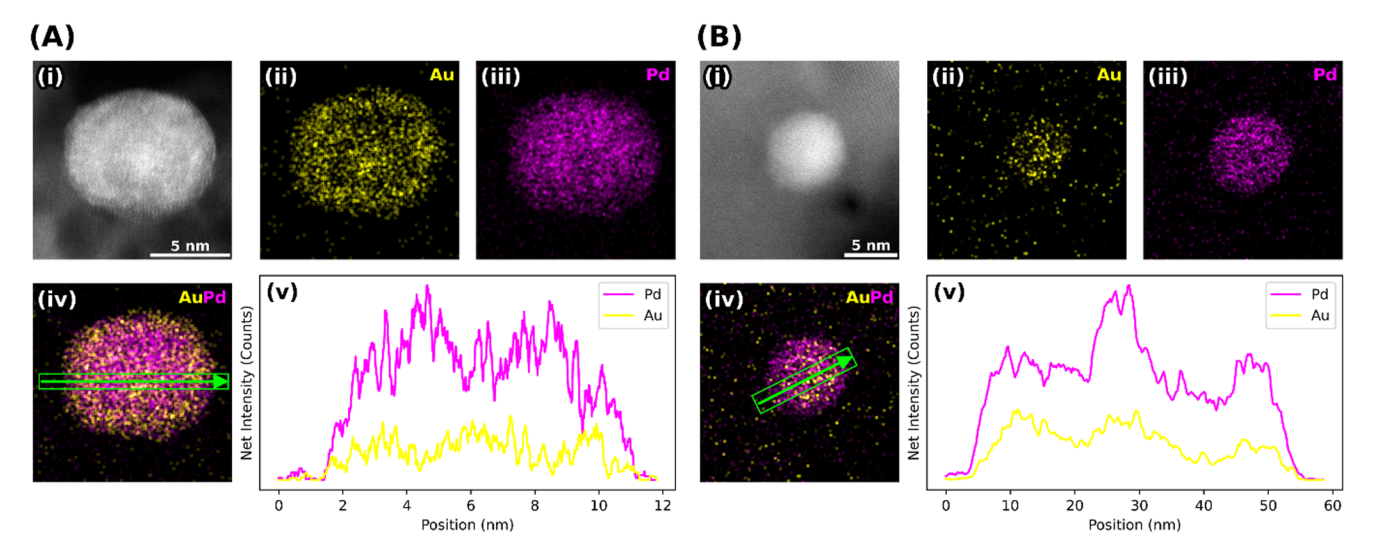


Fig. 2 HAADF-STEM and corresponding EDX analysis of the 0.5%Au-0.5%Pd/TiO₂ catalyst (**A**) before and (**B**) after use in the oxidative degradation of phenol (50 h). *Key*: Au (*yellow*), Pd (*magenta*).

Reaction conditions: catalyst (0.12 g), SiC (4.1 g), phenol solution (10 ppm, in $\rm H_2O$), total gas flow rate: 42 mLmin⁻¹ ($\rm H_2:O_2=1$), 10 bar, liquid flow rate: 0.2 mLmin⁻¹, 20 °C

reagent contact time, as indicated by the higher rates of oxidative degradation observed at slower liquid and gaseous flow rates (Fig. 3A, B) and the direct correlation between substrate conversion and reaction pressure (Fig. 3C), which is consistent with the reported first-order dependence of $\rm H_2O_2$ formation rates on $\rm H_2$ partial pressures [30]. Importantly, a direct correlation between catalyst mass and phenol conversion was observed, with rates of phenol degradation approaching 100% observed when utilising a catalyst mass of 0.24 g (Fig. 3D).

Legislation regulating phenolic compounds in water bodies is becoming increasingly stringent, with legal limits in the European Union ranging from 0.5 ppb in drinking water to 8 ppb in surface water [31, 32]. Although our initial studies demonstrated effective phenol degradation at much higher concentrations (10 ppm) than those permitted by law, we were motivated to explore the limitations of this technology. With an aim to assess its potential for application in the treatment of chemical waste streams, where phenol concentrations are significantly higher, we evaluated system performance (with a fixed catalyst mass of 0.12 g) at levels of phenol as high as 50 ppm (i.e. 100000 times greater than that permitted in drinking water) (Fig. 4A). Unsurprisingly, we observed a reduction in phenol conversion as phenol concentration increased. However, the in-situ approach was still able to achieve conversion rates as high as 40% (at a phenol concentration of 50 ppm), with no loss in catalyst performance observed on-line. Notably, in the case of these experiments we were able to quantify the products of phenol degradation (Figure S.12), which was not possible for our earlier studies where a phenol concentration of 10 ppm was utilised and limits of detection of our analysis equipment prohibited our establishment of product selectivity. Importantly, we observe a relatively high selectivity towards the highly oxidized products (i.e. the combined acids, CO₂ and H₂O which are grouped as "others" in Figure S.12), rather than the phenolic derivates (catechol, resorcinol, etc.), which is highly promising given that many of the phenolic derivatives pose a greater health concerns than phenol itself.

Building on this observation we subsequently evaluated catalytic efficacy towards the degradation of phenolic derivatives; hydroquinone, catechol, benzoquinone, and resorcinol (Fig. 4B). Relatively high (>85%) rates of conversion were observed, somewhat higher than those observed for phenol itself, with such data clearly indicating the relative variation in the efficacy of reactive oxygen species towards the degradation of the various derivatives. However, these observations perhaps reveal the promise of the in-situ approach to pollutant remediation.

4 Conclusions

We have demonstrated that the introduction of Au into supported Pd catalysts can enhance catalytic performance, not only towards the direct synthesis of H_2O_2 but also the oxidative degradation of phenol via in-situ production of H_2O_2 and associated reactive oxygen species. This is observed



373 Page 10 of 12 R.-J. Li et al.

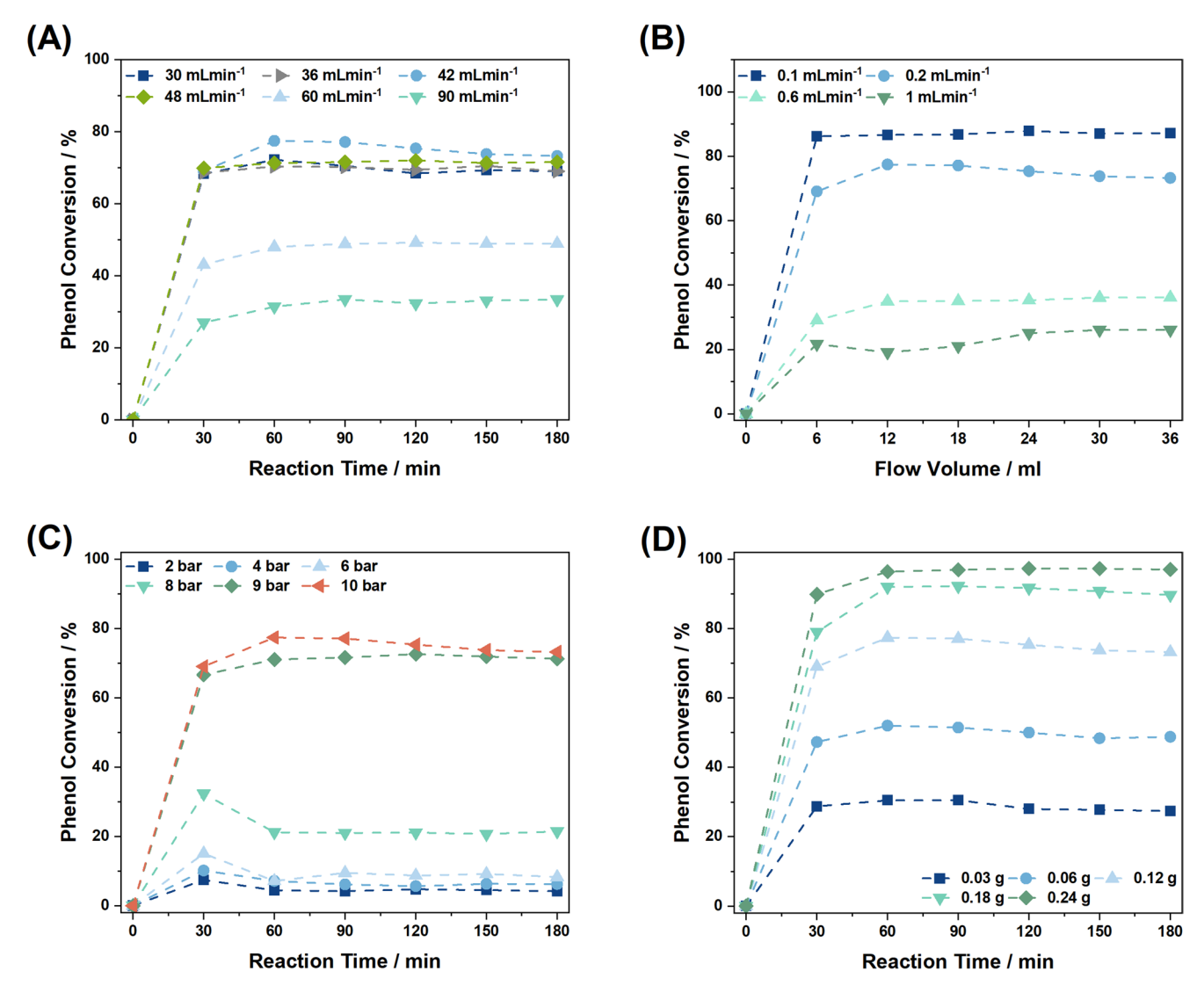


Fig. 3 Optimisation of reaction conditions for the in-situ oxidative degradation of phenol over the 0.5%Au-0.5%Pd/TiO₂ catalyst. (**A**) The effect of gas and (**B**) liquid flow rates as well as (**C**) total gas pressure and (**D**) catalyst loading on phenol degradation. Reaction condi-

tions: catalyst (0.03–0.24 g), SiC (4.1 g), phenol solution (10 ppm, in $\rm H_2O$), total gas flow rate: 30–90 mLmin⁻¹, total pressure 2–10 bar, total liquid flow rate: 0.1–1.0 mLmin⁻¹ 20 °C

under reaction conditions where conversion is limited when using commercial $\rm H_2O_2$. Through optimisation of key reaction parameters, phenol degradation rates approaching 100% may be achieved, with high efficacy towards the mineralisation of phenolic degradation products also observed. Importantly, the optimal 0.5%Au-0.5%Pd/TiO₂ catalyst was found to be highly stable, with no loss in catalyst

performance observed over 50 h on-stream, although we recognise the need for further efforts to prevent the agglomeration of active species under prolonged use. We consider that these catalysts represent a promising basis for further exploration for the oxidative degradation of a range of recalcitrants.



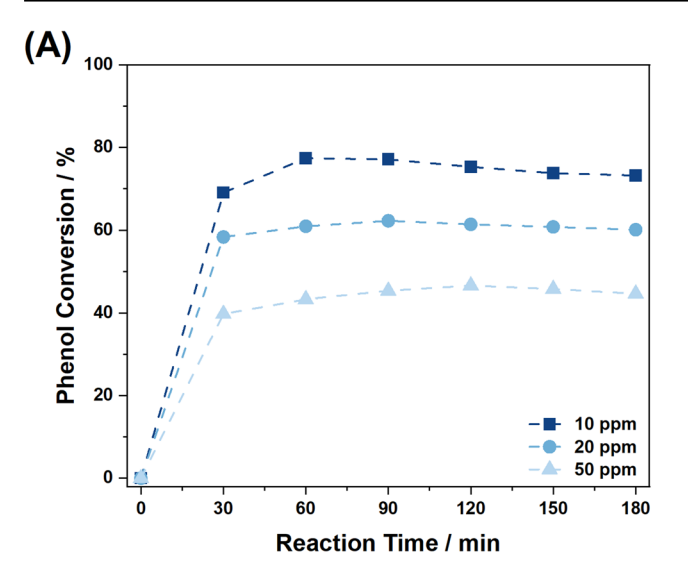


Fig. 4 Catalytic activity towards the oxidative degradation of (A) phenol, as a function of phenol concentration and (B), phenol oxidation products. Reaction conditions: catalyst (0.12 g), SiC (4.1 g), phenol

Supplementary Information The online version contains supplementary material available at https://doi.org/10.1007/s10562-025-05221-3.

Acknowledgements The authors wish to thank the Cardiff University electron microscope facility (CCI-EMF), which has been part-funded by the European Regional Development Fund through the Welsh Government and The Wolfson Foundation for the transmission electron microscopy. XPS data collection was performed at the EPSRC National Facility for Photoelectron Spectroscopy ("HarwellXPS", EP/Y023587/1, EP/Y023609/1, EP/Y023536/1, EP/Y023552/1 and EP/Y023544/1). Funding: R.L acknowledges the Chinese Scholarship Council for funding. R.J.L, N.F.D and G.J.H are grateful to The Max Planck Centre for Fundamental Heterogeneous Catalysis (FUNCAT) for financial support.

Author Contributions R. L, and R. J. L conducted testing experiments and corresponding data analysis. R. L, D. J. M and E.A conducted catalyst characterization and corresponding data processing. R. J. L, N.F.D and G. J. H contributed to the design of the study. R. J. L, N.F.D, T.S and G. J. H provided technical advice and result interpretation. R.J.L wrote the Manuscript and Supporting Information, with all authors commenting on and amending both documents. All authors discussed and contributed to the work agree to its submission.

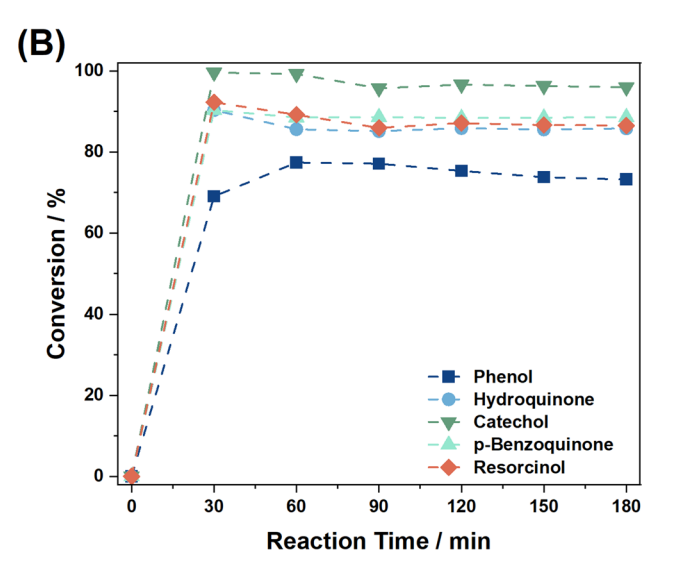
Funding R.L acknowledges the Chinese Scholarship Council for funding. R.J.L, N.F.D and G.J.H are grateful to The Max Planck Centre for Fundamental Heterogeneous Catalysis (FUNCAT) for financial support.

Data Availability The authors declare that the data supporting the findings of this study are available within the paper and its Supplementary Information files.

Declarations

Competing Interests The authors declare no competing interests.

Ethical and Consent to Participate Not Applicable.



solution (10–50 ppm, 10 ppm in the case of the phenolic derivatives in $\rm H_2O$), total gas flow rate: 42 mLmin⁻¹ ($\rm H_2:O_2=1$), 10 bar, liquid flow rate: 0.2 mLmin⁻¹, 20 °C

Consent for Publication Not Applicable.

Open Access This article is licensed under a Creative Commons Attribution 4.0 International License, which permits use, sharing, adaptation, distribution and reproduction in any medium or format, as long as you give appropriate credit to the original author(s) and the source, provide a link to the Creative Commons licence, and indicate if changes were made. The images or other third party material in this article are included in the article's Creative Commons licence, unless indicated otherwise in a credit line to the material. If material is not included in the article's Creative Commons licence and your intended use is not permitted by statutory regulation or exceeds the permitted use, you will need to obtain permission directly from the copyright holder. To view a copy of this licence, visit https://creativecommons.org/licenses/by/4.0/.

References

- Grace Pavithra K, Sundar Rajan P, Arun J, Brindhadvei K, Le QH, Pugazhendhu A (2023) A review on recent advancements in extraction, removal and recovery of phenols from phenolic wastewater: challenges and future outlook. Environ Res 237:117005
- Han X, Chang H, Wang C, Tai J, Karellas S, Yan J, Song L, Bi Z (2023) Tracking the life-cycle greenhouse gas emissions of municipal solid waste incineration power plant: A case study in Shanghai. J Clean Prod 398:136635
- Christensen ML, Keiding K, Nielsen PH, Jørgensen MK (2015) Dewatering in biological wastewater treatment: a review. Water Res 82:14–24
- Narayanan CM, Narayan V (2019) Biological wastewater treatment and bioreactor design: a review. Sustain Environ Res 29:33
- Hussain A, Kumari R, Sachan SG, Sachan A (2021) Chap. 8 -Biological wastewater treatment technology: advancement and drawbacks. In: Shah M, Rodriguez-Couto S (eds) Microbial ecology of wastewater treatment plants. Elsevier, Amsterdam, pp 175–192
- 6. Chen Y, Ren W, Ma T, Ren N, Wang S, Duan W (2024) Transformative removal of aqueous micropollutants into polymeric



373 Page 12 of 12 R.-J. Li et al.

- products by advanced oxidation processes. Environ Sci Technol 58:4844–4851
- Wu J, Yu H (2024) Confronting the mysteries of oxidative reactive species in advanced oxidation processes: an elephant in the room. Environ Sci Technol 58:18496–18507
- Zhang Q, Zheng D, Bai B, Ma Z, Zong S (2024) Insight into antibiotic removal by advanced oxidation processes (AOPs): Performance, mechanism, degradation pathways, and ecotoxicity assessment. Chem Eng J 500:157134
- Kato S, Kansha Y (2024) Comprehensive review of industrial wastewater treatment techniques. Environ Sci Pollut Res 31:51064–51097
- Liu S, Ma Q, Wang B, Wang J, Zhang Y (2014) Advanced treatment of refractory organic pollutants in petrochemical industrial wastewater by bioactive enhanced ponds and wetland system. Ecotoxicology 23:689–698
- Wang J, Chen H (2020) Catalytic ozonation for water and wastewater treatment: recent advances and perspective. Sci Total Environ 704:135249
- Lewis RJ, Hutchings GJ (2019) Recent advances in the direct synthesis of H₂O₂. ChemCatChem 11:298–308
- 13. He J, Lv Z, Su M, Pu Y, Song W, Gao J, Yuan S, Wang Y, Ouyang L (2025) Direct synthesis of $\rm H_2O_2$ over Pd-In/TiO $_2$ and in situ activation toward Tetracycline degradation. Mater Res Bull 192:113584
- Underhill R, Lewis RJ, Freakley SJ, Douthwaite M, Miedziak PJ, Akdim O, Edwards JK, Hutchings GJ (2018) Oxidative degradation of phenol using in situ generated hydrogen peroxide combined with fenton's process. Johnson Matthey Technol Rev 62:417–425
- Santos A, Lewis RJ, Morgan DJ, Davies TE, Hampton E, Gaskin P, Hutchings GJ (2021) The degradation of phenol via in situ H₂O₂ production over supported Pd-based catalysts. Catal Sci Technol 11:7866–7874
- Richards T, Harrhy JH, Lewis RJ et al (2021) A residue-free approach to water disinfection using catalytic in situ generation of reactive oxygen species. Nat Catal 4:575–585
- Santos A, Lewis RJ, Morgan DJ, Davies TE, Loveridge EJ, Crole DA, Edwards JK, Gaskin P, Kiely CJ, He Q, Murphy DM, Maillard J, Freakley SJ, Hutchings GJ (2022) The oxidative degradation of phenol via in situ H₂O₂ synthesis using Pd supported Fe-modified ZSM-5 catalysts. Catal Sci Technol 12:2943–2953
- Neyens E, Baeyens J (2003) A review of classic fenton's peroxidation as an advanced oxidation technique. J Hazard Mater 98:33-50
- Ntainjua EN, Edwards JK, Carley AF, Lopez-Sanches JA, Moulijin JA, Herzing AA, Kiely CJ, Hutchings GJ (2008) The role of the support in achieving high selectivity in the direct formation of hydrogen peroxide. Green Chem 10:1162–1169
- Wilson NM, Priyadarshini P, Kunz S, Flaherty DW (2018) Direct synthesis of H₂O₂ on Pd and Au_xPd₁ clusters: understanding the effects of alloying Pd with Au. J Catal 357:163–175

- Gudarzi D, Ratchananusorn W, Turunen I, Heinonen H, Salmi T (2015) Promotional effects of Au in Pd–Au bimetallic catalysts supported on activated carbon cloth (ACC) for direct synthesis of H₂O₂ from H₂ and O₂. Catal Today 248:58–68
- Edwards JK, Ntainjua NE, Carley AF, Herzing AA, Kiely CJ, Hutchings GJ (2009) Direct synthesis of H₂O₂ from H₂ and O₂ over gold, palladium, and gold–palladium catalysts supported on acid-pretreated TiO₂. Angew Chem Int Ed 48:8512–8515
- Sharp G, Lewis RJ, Liu J, Magri G, Morgan DJ, Davies TE, López-Martín Á, Li R, Morris CR, Murphy DM, Folli A, Dugulan AI, Chen L, Liu X, Hutchings GJ (2024) Benzyl alcohol valorization via the in situ production of reactive oxygen species. ACS Catal 14:15279–15293
- Sharp G, Lewis RJ, Magri G, Liu J, Morgan DJ, Davies TE, López-Martín Á, Murphy DM, Folli A, Chen L, Liu X, Hutchings GJ (2025) Highly efficient benzyl alcohol valorisation via the in situ synthesis of H₂O₂ and associated reactive oxygen species. Green Chem 27:5567–5580
- Garcia-Segura S, Brillas E (2024) Redesigning electrochemicalbased Fenton processes: an updated review exploring advances and innovative strategies using phenol degradation as key performance indicator. Appl Catal O-Open 194
- 26. Tian P, Ouyang L, Xu X, Ao C, Xu X, Si R, Shen X, Lin M, Xu J, Han F (2017) The origin of palladium particle size effects in the direct synthesis of H₂O₂: is smaller better? J Catal 349:30–40
- Brehm J, Lewis RJ, Morgan DJ, Davies TE, Hutchings GJ (2022)
 The direct synthesis of hydrogen peroxide over AuPd nanoparticles: an investigation into metal loading. Catal Lett 152:254–262
- Li R, Lewis RJ, López-Martín Á, Morgan DJ, Davies TE, Kordus D, Dugulan AI, Cuenya BR, Hutchings GJ (2025) Promoting H₂O₂ direct synthesis through Fe incorporation into AuPd catalysts. Green Chem 27:2065–2077
- 29. Kovačič D, Lewis RJ, Crombie CM, Morgan DJ, Davies TD, López-Martín Á, Qin T, Allen CS, Edwards JK, Chen L, Skjøth-Rasmussen MS, Liu X, Hutchings GJ (2023) A comparative study of palladium-gold and palladium-tin catalysts in the direct synthesis of H₂O₂. Green Chem 25:10436–10446
- Liu Q, Lunsford JH (2006) Controlling factors in the direct formation of H₂O₂ from H₂ and O₂ over a Pd/SiO₂ catalyst in ethanol. Appl Catal A Gen 314:94–100
- Jiang H, Fang Y, Fu Y, Guo Q (2003) Studies on the extraction of phenol in wastewater. J Hazard Mater 101:179–190
- European Commission (2023) Drinking water Improving access to drinking water for all, via https://environment.ec.europa.eu/top ics/water/drinking-water_en. Accessed 28 Aug 2025

Publisher's Note Springer Nature remains neutral with regard to jurisdictional claims in published maps and institutional affiliations.

